ELSEVIER

Biophysical Chemistry 126 (2007) 50–58

Biophysical Chemistry

http://www.elsevier.com/locate/biophyschem

The thermodynamics of vinca alkaloid-induced tubulin spirals formation

Sharon Lobert [a,b], Jeffrey W. Ingram [b], John J. Correia [b,*]

[a] School of Nursing, University of Mississippi Medical Center, Jackson, MS 39216, United States
[b] Department of Biochemistry, University of Mississippi Medical Center, 2500 N. State St., Jackson, MS 39216, United States

Received 8 March 2006; received in revised form 22 May 2006; accepted 22 May 2006
Available online 6 June 2006

Abstract

Vinca alkaloids are antimitotic, anticancer agents that induce tubulin to form spiral polymers at physiological protein concentrations. We used sedimentation velocity to investigate the effects of six vinca alkaloids on tubulin spiraling. Fitting to a Wyman linkage model reveals a drug dependent change of over two orders of magnitude in spiraling potential, K_1K_2. Thermodynamic analysis of $\mathrm{Ln}K_1K_2$ data demonstrates large and positive ΔS values, indicating that tubulin spiral formation is entropically-driven. From the curvature in van't Hoff plots of vinblastine data, we estimate ΔC_p for GTP and GDP conditions to be −439 and −396 cal/mol K. Partitioning of ΔS into the hydrophobic effect, ΔS_{HE}, change in rotational/translational freedom, ΔS_{RT} and change in protein conformation, ΔS_{other}, demonstrates that the major driving force for tubulin spiral formation is burial of hydrophobic surfaces and that protein conformational changes do not make a significant contribution. Spiraling potential is an indicator of antimitotic activity *in vivo*, although turbidity studies indicate that there is no correlation between spiraling potential and microtubule inhibition *in vitro*. Mechanisms that explain this discrepancy are discussed.

Keywords: Antimitotics; Tubulin; Thermodynamics; Analytical ultracentrifugation

1. Introduction

The vinca alkaloids have been important chemotherapeutic agents since the 1960s. Vincristine, vinblastine and vinorelbine are used in protocols for a wide range of solid and hematologic tumors [1,2] and vinflunine, a new vinca alkaloid, is currently in numerous Phase II clinical trials. These drugs *in vivo* interact with free tubulin and with tubulin in mitotic spindles causing spiral formation and diminished microtubule dynamic instability. Microtubule dynamics are essential for progression through mitosis [3,4]. Application of Wyman linkage theory to this system demonstrates that the overall drug binding affinity is the product of equilibrium constants, K_1K_2, referred to as the spiraling potential, where K_1 describes drug binding to the tubulin heterodimer, and K_2 is the stepwise interaction of liganded-heterodimers to make an indefinite spiral polymer [5]. We have demonstrated that for a group of vinflunine congeners spiraling potential is a predictor of cytotoxicity in L1210 leukemic cells [6]. Furthermore, the magnitude of the spiraling potential, vincristine > vinblastine > vinorelbine > vinflunine [7,8] agrees well with clinical doses, where vincristine < vinblastine < vinorelbine [9].

We present here a thermodynamic analysis of the interaction of six vinca alkaloids with tubulin (Fig. 1). We examined *in vitro* drug binding by sedimentation velocity and microtubule inhibition by turbidity. This class of compounds is comprised of two main chemical moieties, where the upper structure (see Fig. 1) is referred to as the catharanthine moiety and the lower structure as the vindoline moiety. Five of the compounds investigated in this work, vincristine, vinblastine, vindesine, desacetyl-vincristine and desacetyl-desformyl vincristine, were modified on the vindoline moiety and one, vinepidine, on the catharanthine moiety. For completeness of presentation we are

Abbreviations: df-vcr, desformyl vincristine; dadf-vcr, desacetyl-desformyl vincristine; EGTA, [ethylene-bis(oxyethylenenitrilo)]tetraacetic acid; MAP, microtubule associated protein; PC, MAP-free phosphocellulose purified tubulin; Pipes, piperazine-*N*,*N*′-bis(2-ethanesulfonic acid); vcr, vincristine; vfl, vinflunine; vlb, vinblastine; vrb, vinorelbine.

* Corresponding author. Department of Biochemistry, University of Mississippi Medical Center, 2500 N. State St., Jackson, MS 39216, United States. Tel.: +1 601 984 1852.
E-mail address: jcorreia@biochem.umsmed.edu (J.J. Correia).

0301-4622/$ - see front matter © 2006 Elsevier B.V. All rights reserved.
doi:10.1016/j.bpc.2006.05.023

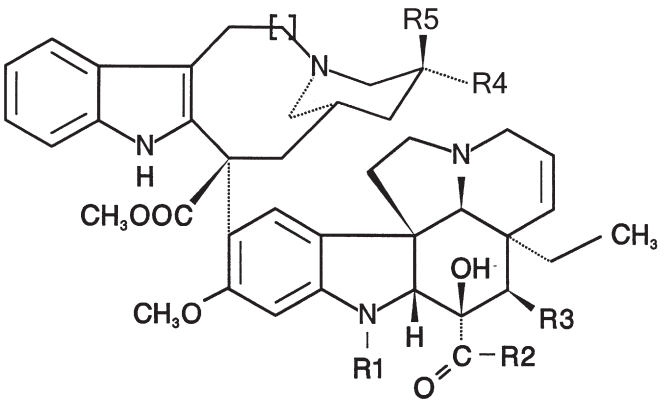

	R1	R2	R3	R4	R5	[ ]
vincristine	CHO	OCH_3	$OCOCH_3$	CH_2CH_3	OH	--
vinblastine	CH_3	OCH_3	$OCOCH_3$	CH_2CH_3	OH	--
vindesine	CH_3	NH_2	OH	CH_2CH_3	OH	--
vinepidine	CHO	OCH_3	$OCOCH_3$	H	CH_2CH_3	--
desformyl-vincristine	H	OCH_3	$OCOCH_3$	CH_2CH_3	OH	--
desacetyl-desformyl-vincristine	H	OCH_3	OH	CH_2CH_3	OH	--
vinorelbine	CH_3	OCH_3	$OCOCH_3$	CH_2CH_3	--	removed
vinflunine	CH_3	OCH_3	$OCOCH_3$	CF_2CH_3	H	removed

Fig. 1. Chemical structures of test compounds.

including the results of sedimentation velocity studies previously carried out for two additional vincas, vinorelbine and vinflunine, modified on the catharanthine moiety [8]. We fit sedimentation velocity data with a Wyman linkage model to obtain precise estimates of overall drug binding and spiraling potential. We present a comparison of ΔG, ΔH, ΔS and ΔC_p derived from these data, indicating that vinca-induced spiral formation is entropically driven via water release and burial of primarily nonpolar surfaces. Protein conformational changes do not contribute significantly to the thermodynamics of spiral growth. Although there is a correlation between spiral potential and antimitotic activity *in vivo* [6], we demonstrate that for these compounds there is no significant correlation between vinca-induced tubulin spiraling potential and microtubule inhibition *in vitro*, and speculate as to the origin of this discrepancy.

2. Materials and methods

2.1. Reagents

Deionized (Nanopure) water was used in all experiments. $MgSO_4$, EGTA[1], GTP (Type II-S), glycerol, Pipes, and vinblastine and vincristine sulfate were purchased from Sigma Chemical Company. Vinorelbine ditartrate was from Glaxo-Wellcome, Inc. Sephadex G-50 was from Pharmacia. The sulfate salts of vindesine, vinepidine, desformyl-vincristine, desacetyl-desformyl-vincristine were a gift from Eli Lilly Co.

2.2. Tubulin purification

Purified tubulin (PC-tubulin) was obtained by warm/cold polymerization/depolymerization. A final phosphocellulose chromatography step was used to separate tubulin from microtubule associated proteins, MAPs [10,11]. Protein concentrations were determined spectrophotometrically using $\varepsilon_{278} = 1.2$ ml/mg cm [12].

2.3. Sedimentation velocity experiments

The effects of vinblastine, vincristine, vinorelbine, vindesine, vinepidine, desformyl-vincristine, and desacetyl-desformyl-vincristine on tubulin spiral formation were studied by sedimentation velocity in the presence of GTP or GDP. Tubulin samples (~2 μM) were equilibrated in 10 mM Pipes, pH 6.9, 2 mM EGTA, 1 mM $MgSO_4$, 50 μM GXP plus the appropriate drug concentration using spun columns. Using this method, the free drug concentration (0.5–70 μM) can be obtained from the compound concentration in the equilibration

Table 1
Equilibrium constants for the interaction of antimitotics with tubulin

Drug	K_1 (M^{-1})	K^2 (M^{-1})	K_1K_2 (M^{-2})	S.D.
GTP, 25 °C				
Vincristine	$1.4\times10^5\pm0.4$	$1.7\times10^7\pm0.4$	2.4×10^{12}	1.2
Vinepedine	$1.0\times10^5\pm2.0$	$2.1\times10^7\pm0.3$	2.1×10^{12}	1.4
Vindesine	$1.2\times10^5\pm0.2$	$9.4\times10^6\pm0.8$	1.1×10^{12}	0.9
Vinblastine	$1.2\times10^5\pm0.2$	$5.1\times10^6\pm0.6$	6.1×10^{11}	0.9
Vinorelbine	$1.3\times10^5\pm0.2$	$1.1\times10^6\pm0.8$	1.4×10^{11}	0.3
DF VCR	$4.4\times10^4\pm0.9$	$1.2\times10^6\pm0.2$	5.3×10^{10}	0.4
DADF VCR	$3.6\times10^4\pm1.1$	$9.7\times10^5\pm2.6$	3.5×10^{10}	0.4
Vinflunine	$8.8\times10^4\pm2.0$	$3.0\times10^5\pm0.4$	2.6×10^{10}	0.2
GDP, 25 °C				
Vincristine	$2.1\times10^5\pm0.4$	$3.9\times10^7\pm0.5$	8.2×10^{12}	1.7
Vinepedine	$1.2\times10^5\pm0.2$	$5.0\times10^7\pm0.5$	6.0×10^{12}	1.7
Vindesine	$1.5\times10^5\pm0.2$	$3.0\times10^7\pm0.3$	4.5×10^{12}	1.6
Vinblastine	$1.3\times10^5\pm0.1$	$2.3\times10^7\pm0.2$	3.0×10^{12}	0.8
Vinorelbine	$1.3\times10^5\pm0.3$	$5.1\times10^6\pm0.6$	6.6×10^{11}	1.0
DF VCR	$4.6\times10^4\pm1.0$	$4.0\times10^6\pm0.7$	1.8×10^{11}	0.7
DADF VCR	$4.7\times10^4\pm1.1$	$3.0\times10^6\pm0.6$	1.4×10^{11}	0.6
Vinflunine	$1.0\times10^5\pm0.3$	$1.2\times10^6\pm0.2$	1.2×10^{11}	0.5

buffer [13]. The following extinction coefficients were used to determine compound concentrations: vinblastine and vindesine $\varepsilon_{320,\ \mathrm{water}}=4647\ M^{-1}\ cm^{-1}$; vincristine, vinepidine, desformyl-vincristine, and desacetyl-desformyl-vincristine $\varepsilon_{296,\ \mathrm{ETOH}}=15{,}136\ M^{-1}\ cm^{-1}$. Sedimentation studies at 5, 15 and 25 °C and appropriate speeds were done in a Beckman Optima XLA analytical ultracentrifuge equipped with absorbance optics and an An60 Ti rotor. In order to calculate the change in heat capacity, ΔC_p, associated with vinca-induced tubulin spiral formation, additional vinblastine experiments were carried out at a total of seven different temperatures between 5 and 37 °C (5, 10, 15, 20, 25, 30, 37 °C) in the presence of GTP or GDP. Data were collected at 278 nm and at a spacing of 0.002 cm with 1 flash of the lamp in a continuous scan mode and were analyzed using software DCDT to generate a distribution of sedimentation coefficients, $g(s)$ [14,15].

2.4. Curve fitting of sedimentation velocity data

The $g(s)$ data were converted to weight average $S_{20,w}$ values as described previously [6,7,13,15] and data (corresponding to 15–18 different drug concentrations) were fit by nonlinear least squares (Fitall, MTR software, Toronto, Canada, modified to include the appropriate fitting functions), using the isodesmic ligand-mediated model to obtain equilibrium constants. K_1 is the affinity of drug for tubulin heterodimers, K_2 is the affinity of liganded-heterodimers for spiral polymers [5,13,15].

2.5. van't Hoff analysis

Sedimentation data collected at 5, 15 and 25 °C were analyzed to obtain the thermodynamic parameters ΔG, ΔH, ΔS. The change in free energy, ΔG, was determined from the natural log of the spiraling potential for ligand-mediated fits of the data, $\mathrm{Ln}K_1K_2$. ΔH was determined from linear regression fits of van't Hoff plots using Origin 5.0, while ΔS was calculated from the relationship $\Delta G=\Delta H-T\Delta S$. The change in heat capacity, ΔC_p, for spiral formation was calculated from the curvature of van't Hoff plots of vinblastine data ($\mathrm{Ln}K_1K_2$ vs. $1/T$) by nonlinear least squares fitting of the data (FITALL, MTR software, Toronto, Canada), as described previously [16]. Limited amounts of the Eli Lilly drugs precluded a complete temperature analysis, but the average behavior of the other seven drugs over a limited temperature range is consistent with the vinblastine van't Hoff analysis.

Table 2
Equilibrium constants for the interaction of vinca alkaloids with tubulin

Drug	K_1 (M^{-1})	K_2 (M^{-1})	K_1K_2 (M^{-2})	S.D.
GTP, 5 °C				
Vincristine	$3.4\times10^5\pm0.8$	$8.0\times10^6\pm0.4$	2.7×10^{12}	1.0
Vinepedine	$9.3\times10^4\pm1.5$	$2.2\times10^7\pm0.2$	2.0×10^{12}	1.1
Vindesine	$1.5\times10^5\pm0.3$	$8.7\times10^6\pm0.8$	1.3×10^{12}	1.0
Vinblastine	$4.7\times10^4\pm1.0$	$4.1\times10^6\pm0.8$	1.9×10^{11}	0.5
Vinorelbine	$7.4\times10^4\pm1.2$	$6.7\times10^5\pm0.7$	5.0×10^{10}	0.2
DF VCR	$8.9\times10^4\pm2.3$	$6.0\times10^5\pm0.9$	5.3×10^{10}	0.4
DADF VCR	$5.1\times10^4\pm0.7$	$8.2\times10^5\pm0.9$	4.2×10^{10}	0.2
Vinflunine	$4.4\times10^4\pm4.3$	$7.3\times10^4\pm5.0$	3.2×10^9	0.2
GDP, 5 °C				
Vincristine	$2.4\times10^5\pm0.5$	$4.0\times10^7\pm0.5$	9.6×10^{12}	1.5
Vinblastine	$1.5\times10^5\pm0.2$	$1.0\times10^7\pm0.1$	1.5×10^{12}	1.0
Vinorelbine	$8.6\times10^6\pm1.6$	$3.8\times10^6\pm0.4$	3.3×10^{11}	0.7
Vinflunine	$9.9\times10^4\pm3.1$	$2.8\times10^5\pm0.4$	2.8×10^{10}	0.2

2.6. Microtubule inhibition

PC-tubulin (1.8 mg/ml) was polymerized in 100 mM Mes, pH 6.9, 10 mM $MgSO_4$, 2 mM EGTA, 1 mM GTP and 2 M glycerol. Experiments in the presence and absence of vinepidine, vindesine, dadf-vcr and df-vcr were done over concentration ranges of 0.1 to 1 μM. For completeness of presentation we also are presenting the effects of compounds previously studied under the same conditions, vincristine, vinblastine, vinflunine and vinorelbine [6]. Turbidity was monitored as a measure of microtubule mass using a Gilford Response II UV–VIS equipped with a cooling Peltier cell holder. Tubulin samples were degassed on ice for 30 min and baseline data were collected

Table 3
Equilibrium constants for the interaction of vinca alkaloids with tubulin

Drug	K_1 (M^{-1})	K_2 (M^{-1})	K_1K_2 (M^{-2})	S.D.
GTP, 15 °C				
Vincristine	$8.7\times10^4\pm1.5$	$2.5\times10^7\pm0.3$	2.2×10^{12}	1.2
Vinepedine	$6.7\times10^4\pm1.3$	$3.1\times10^7\pm0.5$	2.1×10^{12}	1.4
Vindesine	$1.1\times10^5\pm0.3$	$1.4\times10^7\pm0.3$	1.5×10^{12}	1.6
Vinblastine	$8.7\times10^4\pm1.8$	$5.6\times10^6\pm0.8$	4.9×10^{11}	0.9
Vinorelbine	$7.7\times10^4\pm1.8$	$1.3\times10^6\pm0.2$	1.0×10^{11}	0.5
DF VCR	$4.0\times10^4\pm0.1$	$1.6\times10^6\pm0.1$	6.4×10^{10}	0.4
DADF VCR	$3.5\times10^4\pm0.5$	$1.5\times10^6\pm0.2$	5.3×10^{10}	0.2
Vinflunine	$9.7\times10^4\pm3.0$	$1.3\times10^5\pm0.2$	1.3×10^{10}	0.1
GDP, 15 °C				
Vincristine	$1.5\times10^5\pm0.1$	$5.0\times10^7\pm0.2$	7.4×10^{12}	0.8
Vinblastine	$9.3\times10^4\pm2.1$	$2.2\times10^7\pm0.3$	2.0×10^{12}	2.1
Vinorelbine	$1.4\times10^5\pm0.2$	$4.8\times10^6\pm0.3$	6.7×10^{11}	0.5
Vinflunine	$7.4\times10^4\pm1.5$	$8.4\times10^5\pm1.0$	6.2×10^{10}	0.3

at 4 °C and 350 nm. Microtubule formation was initiated by raising the temperature to 37 °C and solutions were monitored at 350 nm for 45 min. Samples were cooled to 0 °C and a second baseline was recorded. Subtraction of the second baseline from the plateau optical density at 45 min was used to calculate the change in optical density, ΔOD. The ΔOD was plotted vs. compound concentration and fit by linear regression using Origin 5.0. The percent inhibition was calculated relative to a control sample in every experiment. The mean of 3 independent experiments was used to estimate the IC_{50} concentration (drug concentration causing 50% inhibition of microtubule assembly) for each test compound (Table 5).

3. Results

3.1. Comparison of vinca-induced tubulin spiraling

Equilibrium constants derived from sedimentation velocity experiments at 25 °C are presented in Table 1. From ligand-mediated fits of the data for the six vindoline-modified compounds (Fig. 1), the overall spiraling potential, K_1K_2 (GTP and GDP data), vary by nearly two orders of magnitude, from the largest values for vincristine (2.4×10^{12} and 8.2×10^{12} M^{-2}) to the smallest for dadf-vcr (3.5×10^{10} and 1.4×10^{11} M^{-2}). When previous data for the catharanthine-modified compounds are included [9], vinflunine demonstrates the smallest spiraling potential (2.6×10^{10} and 1.2×10^{11} M^{-2}). For data collected at 5 and 15 °C in the presence of GTP there is also about two orders of magnitude difference in spiraling potential between the weakest and strongest compound and the same relative ranking of all the compounds (Tables 2 and 3).

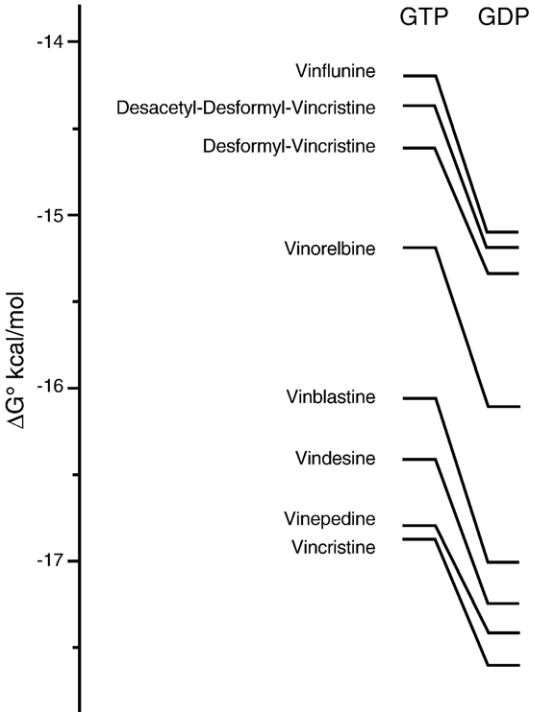

Fig. 2. Free energy of overall spiraling potential ($\Delta G=-RT\mathrm{Ln}K_1K_2$) is plotted for GTP and GDP conditions at 25 °C. K_1K_2 values, determined from ligand-mediated fits, are listed in Table 1. The GDP enhancement is the difference between the GTP and GDP values, with an average value $\Delta\Delta G=0.81\pm0.11$ kcal/mol.

Table 4
Thermodynamic parameters for tubulin–vinca alkaloid interaction at 25 °C

	K_1K_2 (M^{-2})	$\Delta G°$ (kcal/mol)	$\Delta S°$ (cal/mol K)	$\Delta H°$ (cal/mol K)
Vincristine				
GTP	2.7×10^{12}	−16.9	53.4	−1.03
GDP	8.2×10^{12}	−17.6	57.0	−0.62
Vinepidine				
GTP	2.0×10^{12}	−16.8	57.6	+0.40
Vindesine				
GTP	1.1×10^{12}	−16.4	57.5	−0.71
Vinblastine				
GTP	6.1×10^{11}	−16.1	87.6	+10.04
GDP	3.0×10^{12}	−17.0	76.9	+5.91
Vinorelbine				
GTP	1.4×10^{11}	−15.2	80.7	+8.83
GDP	6.6×10^{11}	−16.1	74.2	+5.99
Desformyl-vincristine				
GTP	5.3×10^{10}	−14.6	49.7	+0.20
Desacetyl-desformyl-vincristine				
GTP	3.5×10^{10}	−14.4	43.9	−1.30
Vinflunine				
GTP	2.6×10^{10}	−14.2	108.0	+17.96
GDP	1.2×10^{11}	−15.1	92.5	+12.45

The free energy for spiral formation, ΔG, was determined from the overall spiraling potential, K_1K_2 for ligand-mediated fits of the data. At 25 °C, GDP enhances drug-induced tubulin spiraling by an average of 0.81±0.11 kcal/mol similar to values determine previously for vincas modified uniquely on the catharanthine moiety (0.86±0.23 kcal/mol) [6]. This enhancement due to GDP is shown graphically in Fig. 2. The effect of GDP is additive for each of the compounds studied and we have suggested (see discussion) this facilitates the propagation of spirals into the GDP core of a microtubule, resulting in depolymerization [17,18]. Additional sedimentation velocity experiments were conducted with vincristine and vinblastine at 5 and 15 °C in the presence of GDP, and these data are presented in Tables 2 and 3 along with data previously obtained for vinorelbine and vinflunine [9]. (The four other drugs from Eli Lilly were provided to us in quantities insufficient to do these additional experiments.) The average GDP enhancement in spiraling potential for these four drugs at these lower temperatures (Tables 2 and 3) is similar to the enhancement found at 25 °C, 1.02±0.22 and 0.87±0.16 kcal/mol for the 5 and 15 °C conditions, respectively.

3.2. Thermodynamic analysis of vinca-induced tubulin spiraling

Thermodynamic parameters, $\Delta G°$, $\Delta H°$, and $\Delta S°$, calculated from the overall spiraling potential, K_1K_2, determined from ligand-mediated fits of the data, are presented in Table 4. Spiral

formation is clearly an entropy driven process for all the compounds listed, with large positive $\Delta S°$, ranging from 44 cal/mol K for dadf-vcr to 108 cal/mol K for vinflunine. $\Delta S°$ values determined from GTP data tend to be larger than those determined from GDP data. Only three of the compounds (vinblastine, vinorelbine and vinflunine) demonstrate large and unfavorable $\Delta H°$ for spiral formation (GTP data: 10.04, 8.83 and 17.96 kcal/mol and GDP data: 5.91, 5.99 and 12.45 kcal/mol). For the rest of the compounds, $\Delta H°$ is either slightly negative (−0.62 to −1.30.11 kcal/mol) or slightly positive (0.40 and 0.71 kcal/mol). These relatively unfavorable enthalpies are more than compensated by the favorable positive entropy values.

The correlation of these thermodynamic parameters was examined as shown in Fig. 3. The $\Delta H°$ values are plotted vs. $\Delta S°$ (Fig. 3A) and $\Delta G°$ (Fig. 3B) and fit by linear regression to obtain correlation coefficients, r. Enthalpy–entropy compensation was examined previously for nucleotide effects on microtubule formation, demonstrating that the correlation of thermodynamic parameters is biochemically significant, rather than due to statistical artifact [16]. In the study presented here, the high level of entropy–enthalpy correlation and significance ($r=0.97$, $p<0.0001$, Fig. 3A) for all these compounds indicates that similar processes are involved regardless of the nature of their chemical structure differences. Note that the slope of the $\Delta H°-\Delta S°$ or the compensation temperature ($T_c=314.1\pm17.5$ K or 41.0 °C) is different from the mean temperature over which the parameters were estimated. (Omitting the DF VCR and DADF VCR changes these values to $r=0.99$, $T_c=346.8\pm10.4$ or 73.7 °C.) This is important for identifying chemical vs. non-chemical origins of enthalpy–entropy correlation. The high level of correlation and significance between free energy and enthalpy, $\Delta H°-\Delta G°$, (omitting dadf-vcr and df-vcr: $r=0.80$, $p<0.0005$, Fig. 3B) confirms that the correlation is not statistical in origin but rather due to similar biochemical processes [16].

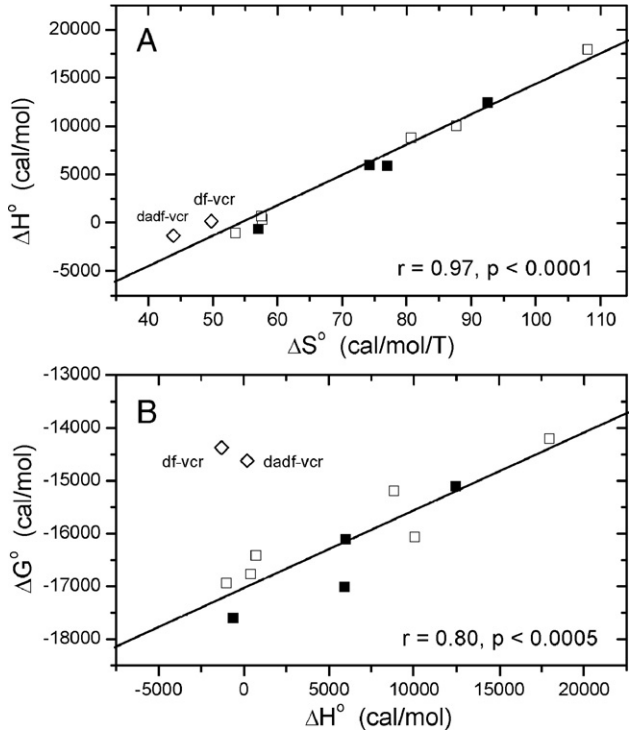

Fig. 3. Plot enthalpy–entropy compensation (A) and free energy–enthalpy compensation. Open symbols are used for GTP data and closed symbols GDP data. Solid lines are the linear regression fits of all the data in (A) and for data without df-vcr and dadf-vcr in (B).

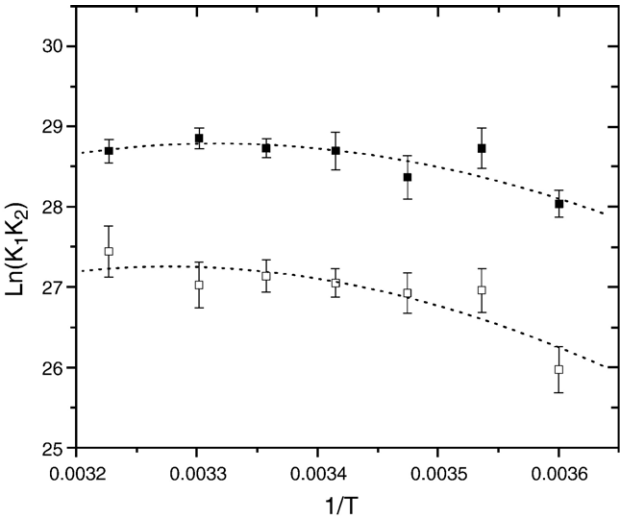

Fig. 4. van't Hoff plots of GTP (open symbols) and GDP (closed symbols) data for vinblastine. Lines represent nonlinear regression fits of the data to obtain ΔC_p values of −396 cal/mol K for GDP conditions and −439 cal/mol K for GTP conditions.

In order to estimate the magnitude of water release and the change in water accessible surface area (ASA) occurring with spiral formation, ΔC_p was determined from vinblastine data collected at multiple temperatures between 5 and 37 °C in the presence of GTP or GDP (Fig. 4). As shown in Fig. 4, the van't Hoff plots have a slight curvature resulting in a negative ΔC_p ascribed to the release of water as water accessible surface areas (ASA) are buried [16,17]. The larger negative value for ΔC_p found in the presence of GTP, −439 cal/mol K, is statistically indistinguishable from the value measured in the presence of GDP, −396 cal/mol K. Nonetheless, the burial of both nonpolar and polar accessible surfaces is likely to contribute to this process [16]. Increasing NaCl or ionic strength was previously found to have a greater effect on vinblastine-induced tubulin spiral formation in the presence of GTP compared to GDP, suggesting an inhibitory effect of charged surfaces under GTP-bound conditions [7,19].

Table 5
Microtubule inhibition

	IC_{50} (μM) [a]
Vinblastine [b]	0.366 (±0.07)
Vinepidine	0.415 (±0.04)
Vinorelbine [b]	0.437 (±0.04)
Vincristine [b]	0.445 (±0.06)
Vinflunine [b]	0.486 (±0.05)
Vindesine	0.497 (±0.03)
Desformyl-vincristine	0.714 (±0.14)
Desacetyl-desformyl-vincristine	0.750 (±0.02)

[a] Drug concentration for 50% inhibition of microtubule mass.
[b] Data from [6].

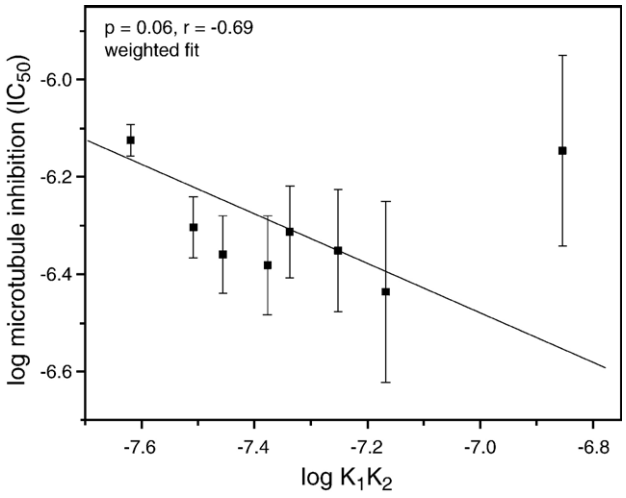

Fig. 5. Plot of log microtubule inhibition vs. log K_1K_2 for sedimentation velocity data collected in the presence of GTP. Data were fit by linear regression using Origin 5.0 to obtain p and r, the correlation coefficient.

3.3. Vinca inhibition of microtubule polymerization

The effect of each of the compounds on microtubule formation was studied by measuring turbidity at 350 nm as a function of test compound concentration. Absorbance in solutions of pure tubulin under polymerizing conditions at this wavelength is determined by microtubule mass. Table 5 presents IC_{50} values, drug concentrations that inhibited microtubule polymer formation by 50%, for each of the eight compounds. The vincristine, vinblastine, vinflunine and vinorelbine values were reported previously and are reported here for completeness of presentation [6]. The values range from 0.366±0.07 μM for vinblastine to 0.750±0.02 μM for dadf-vcr. However most IC_{50} values fall within a fairly narrow range, (average=0.514±0.141) with only two that are greater than 0.497 μM. Thus it is not surprising that there is no significant correlation between these data and spiraling potential, log K_1K_2 (Fig. 5). The linear regression fit of the data, weighted by the standard deviations, gives a p value of 0.06 (relative to slope=0) and a correlation coefficient of −0.69, while examination of the plot suggests one should be cautious in concluding that there is a meaningful correlation. This result agrees with our previous study of vincas modified on the catharanthine moiety [6] and we conclude that vinca-induced spiraling inhibits microtubule polymerization *in vitro* to the same extent for each drug when performed at stoichiometric drug concentrations (see Discussion).

4. Discussion

4.1. Comparison of vinca alkaloid-induced tubulin spiraling potential, K_1K_2

It was previously demonstrated in studying vinca alkaloid effects on tubulin spiraling, that the catharanthine moiety or the upper half of the vinca alkaloid structure (Fig. 1) alone can achieve 70% of the effect of the parent compound [20]. Note that the catharanthine structure in this previous work was in fact different from the rearranged cleavamine in the vinca alkaloid structure (Fig. 1). The vindoline moiety alone (lower half) did not induce tubulin spirals, and these authors, therefore, suggested it may be important in anchoring the drug molecule. In the work reported here, the effects of vinca alkaloid chemical differences (primarily on the vindoline moiety) on tubulin spiraling potential can be examined relative to vinblastine by comparing the change in free energy, $\Delta\Delta G$, for spiral formation determined from $\mathrm{Ln}K_1K_2$ (Fig. 2). Three of the compounds were more effective than vinblastine in inducing spiral formation and four were less effective. The compound most similar to vinblastine is vindesine where the R2 methyl-ester on the vindoline moiety is replaced by an amino group, resulting in slightly enhanced tubulin spiral formation, $\Delta\Delta G=-0.349$ kcal/mol. For both vincristine and vinepidine, tubulin spiraling potential is enhanced significantly by replacing the vindoline R1 methyl group with a formyl group, $\Delta\Delta G=-0.810$ and -0.731 kcal/mol, respectively. Note that vinepidine has additional changes on the catharanthine moiety at R4 and R5. We have previously described this as an important part of the molecule, potentially interacting directly with tubulin side chains via hydrogen bonding [6]. Thus it is not surprising that changes in this region found in vinepidine can reduce the spiraling potential relative to vincristine. The other two compounds that are modified uniquely on the vindoline moiety are df-vcr and dadf-vcr. Both demonstrate considerably weaker effects on tubulin spiraling relative to vinblastine ($\Delta\Delta G=+1.446$ and $+1.692$ kcal/mol respectively), apparently due to the removal of the R1 methyl group. The difference between df-vcr and dadf-vcr is the removal of the acetyl group from the R3 position in dadf-vcr, suggesting that R3, as well as R1 may interact with tubulin. Vinorelbine and vinflunine differ from vinblastine by modifications in the catharanthine moiety that have been discussed previously. They demonstrate weaker tubulin spiraling potential relative to vinblastine, +0. 871 and +1.868 kcal/mol. Both have the hydroxyl removed at R5 and a carbon removed from the 8 membered ring. However, saturation of the double bond in vinflunine between C3′ and C4′ and the difluorination at R4 significantly reduce its ability to induce tubulin spiraling compared to vinorelbine. As discussed above for vinepidine, we have hypothesized that the modifications at the R4 and R5 positions that affect hydrogen bonding can enhance or inhibit spiral formation [6].

In summary, previous work demonstrated the importance of the catharanthine moiety in affecting tubulin spiral size. The work reported here indicates that hydrogen bonding may also occur between tubulin and the vindoline moiety R1 position, since the formyl group in vincristine or vinepidine enhances tubulin spiraling. Our work suggests that hydrogen bonding via the R1 position formyl group significantly favors the "anchoring' activity of the vindoline moiety. The work reported here also confirms the significance of the R5 position, where an ethyl group in vinepidine disfavors spiral formation relative to vincristine.

4.2. Thermodynamic analysis of vinca alkaloid-induced tubulin spiral formation

Enthalpy–entropy and enthalpy–free energy analysis demonstrates that these parameters are highly correlated (Fig. 3A and B). This high level of correlation (r=0.97 and 0.80) indicates that for these compounds similar biochemical processes are involved in the induction of tubulin spirals. The correlation coefficient for $\Delta H°$–$\Delta G°$ was determined without the two outliers in Fig. 3B, df-vcr and dadf-vcr. The reason for the relative lack of correlation for these two compounds is not clear. It is possible that the R1 position, which appears to be important in anchoring the compound, may also play a significant role in the biochemical processes of spiral formation. An anchoring function is consistent with the 2–4 fold smaller K_1 values for these compounds relative to the other drugs. However, this alone does not account for the 3 kcal/mol smaller ΔG values determined for these compounds. Alternatively other factors like drug solubility may contribute to the unfavorable free energy or the more favorable enthalpy observed.

The positive entropy and small enthalpy values in Table 4 indicate that spiral formation is largely an entropically driven phenomenon mediated by the release of water molecules. Larger entropy values in the presence of GTP compared to GDP support previous experiments where Wyman linkage analysis demonstrated a greater change in NaCl binding in the presence of GTP compared to GDP, suggesting an inhibitory effect on spiral formation for GTP-tubulin due to charge–charge interactions [19]. This is verified by our previous results that demonstrate the thermodynamics of assembly are sensitive to ionic conditions [16]. Nonetheless similar structural changes for vinblastine-induced spiral formation of GTP- and GDP-tubulin are suggested by the similar and larger negative change in heat capacity, ΔC_p (−439 ca/mol K and −396 cal/mol K; Fig. 4). From the ΔC_p we can estimate the change in water accessible surface area as tubulin spirals polymerize. The work of Spolar et al. demonstrated that the buried nonpolar surface area (ΔA_{np}) can be estimated from ΔA_{np}=4.21ΔC_p [16,21,22]. This relationship gives a buried nonpolar surface area of 1667 and 1848 A^2 for GDP and GTP conditions. These values are close to the estimated total ASA burial, polar and nonpolar surfaces, as a single microtubule protofilament polymerizes, 1963 A^2 [16], and the difference may be attributed to conformational changes and the burial of polar surfaces, ΔA_p=115–296 A^2 in the microtubule lattice.

The interpretation of enthalpy–entropy compensation as being due to the release of bound water is not without pitfalls [23]. As described above statistical artifacts due to experimental limitations and trivial mathematical linkages are possible [16,23]. In addition numerous studies have concluded that changes in free energy are far more reliable for simply analysis of molecular interactions than changes in enthalpy [24,25]. In general there is no correlation between enthalpy and free energy changes for protein folding and peptide binding studies [24]. In the comparison presented here, all of the vinca alkaloids are similar chemical moieties interacting with the same protein–protein interface to produce spiral polymer distributions that exhibit similar thermodynamic profiles. While other noncovalent interactions may sum to give rise to similar thermodynamic features, the simplest interpretation of the data is that the linkage between enthalpy and entropy reflect cooperative interactions at the tubulin–vinca alkaloid–tubulin interface [26]. A prominent role for the hydrophobic effect is supported by the observation (Fig. 3B) that the free energy of spiral formation correlates with the change in enthalpy for 10 of the 12 drugs investigated in this study. Thus, while other factors undoubtedly contribute, the major driving force for spiral assembly is the hydrophobic effect and the release of bound water. A similar extra-thermodynamic assignment has been made for example in the underlying linkage between enthalpy and entropy for the family of DIP based DNA binding compounds described elsewhere in this honorary volume [27]. A direct measure of the number of water molecules released during spiral formation, done as a function of osmolyte concentration and water activity, would provide additional and convincing evidence for this interpretation. This type of study is not without problems since osmolytes are known to alter the mode of association, the quaternary structure, of ligand-induced tubulin polymers. Nonetheless, we hope to present these experimental results elsewhere.

4.3. Entropy analysis of vinca-induced spiral formation

The thermodynamic data can be further analyzed by calculating the contributions to the entropy values for vinblastine-induced tubulin spiral formation in Table 4: the hydrophobic effect, ΔS_{HE}, the change in rotational/translational freedom, ΔS_{RT} and the change in conformational entropy, ΔS_{other} (Table 6) [16,22]. As discussed above, from the curvature in the plots in Fig. 4, the change in heat capacity, ΔC_p can be determined, permitting the calculation of T_s, where ΔS is equal to zero for GTP and GDP conditions, 355 and 372 K. The hydrophobic contribution, $\Delta S_{HE}(T_s)$ can be determined from $\Delta S_{HE}(T_s)=1.35\times\Delta C_p\ln(T_s/386)$ [22]. Assuming that the loss of translational and rotational freedom is the same for all association reactions, the ΔSRT is estimated to be −50 cal/mol K [16,22]. When ΔS=0, ΔS_{other}, determined from $\Delta S(T_s)=0=\Delta S_{HE}(T_s)+\Delta S_{rt}+\Delta S_{other}$ [22], is +30 and 0 cal/mol K for GDP and GTP conditions. These small values are to be compared with our previous estimates for GTP-induced (−115 to −235 cal/mol K) and GMPCPP-induced (−348 to −679 cal/mol K) microtubule assembly [16]. When

Table 6
Entropic contributions to vinblastine-induced tubulin spiral formation

GXP	ΔC_p (cal/mol K)	T_s [a] (K)	S_{HE} [b] (cal/mol K)	ΔS_{RT} [c] (cal/mol K)	ΔS_{other} [d] (cal/mol K)
GDP	−396	372	20	−50	+30
GTP	−439	355	50	−50	0

[a] Calculated from 24.7 °C at ΔS=0 [16,22].
[b] Calculated from $\Delta S_{HE}(T_s)=1.35\Delta C_p\ln(T_s/386)$ [16,22].
[c] From [16,22].
[d] Calculated from $\Delta S(T_s)=0=\Delta S_{HE}(T_s)+\Delta S_{rt}+\Delta S_{other}$ [16,22].

converted to organization per amino acid, the data for vinblastine-induced assembly correspond to 0 to 5 amino acids disorganized versus 20 to 120 amino acids organized for microtubule assembly [16,22]. This interpretation is equally consistent with the lattice model, cooperative order–disorder transition calculated by Cooper et al. [23]. Thus, these results suggest vinca-induced spiral formation can be modeled as rigid body associations, with no net folding or unfolding of the protein. We cannot however rule out the possibility that protein conformational changes are compensated by drug conformational changes.

4.4. Implications for drug cytotoxicity

We previously demonstrated that for a group of vinflunine derivatives, tubulin spiral formation correlates with cytotoxicity in L1210 leukemic cells [6]. In that work we also showed that although *in vitro* microtubule inhibition by vincas suggests drug activity, it is not a good predictor of cellular structure–activity relationships. In the work reported here we also found that for these compounds spiral size does not predict *in vitro* microtubule inhibition IC_{50} values. Thus we conclude that although tubulin spirals can act as a buffer or sink for vinca molecules and therefore compounds that induce larger spirals may be more cytotoxic, spiral size alone does not mediate microtubule inhibition *in vitro*. Recently we have shown in cyro EM 15 protofilament microtubule reconstruction studies [28] that vinblastine can bind directly to the microtubule lattice at or near the inter-dimer interface [26]. To observe this taxol must be present to prevent microtubule disassembly. (Extremely weak binding of vinblastine to microtubules, $3–4\times10^3$ M^{-1} , has been reported before [29,30] but the nature of the polymer distribution in the presence of vinca alkaloids was uncertain and precluded a definitive assignment of the binding site or sites.) Thus, microtubule inhibition *in vitro* appears to require destabilization of the microtubule lattice by direct binding to the inter-dimer interface in addition to a competing equilibrium with vinca alkaloid-induced spiral polymers. This explains the nearly stoichiometric and constant magnitude of the *in vitro* IC_{50} values (see Table 5). Vinca alkaloid induced mitotic arrest in cells occurs in the absence of microtubule depolymerization [4], and thus these drugs must target with high affinity other *in vivo* processes that are more sensitive to the spiral forming mode of action of these drugs [6,17,18]. These other processes are typically categorized as effects on microtubule dynamics at microtubule ends [3,4], but interactions with other regulatory factors are also potential sites of interaction [17,18,31]. Current studies in our laboratory are investigating the interaction of microtubule regulatory factors (i.e., stathmin and tau) with tubulin and vinca alkaloids.

Acknowledgements

This work was supported by UMMC AUC Facility and NIH Grant NR04780. We dedicate this work to the inspiration and leadership of Julian Sturtevant whose fundamental studies in thermodynamics and calorimetry lead the way for all of us.

References

[1] P. Calabresi, B.A. Chabner, in: J.G. Hardman, L.E. Limbird, P.B. Molinoff, R.W. Ruddor, A. Goodman Gilman (Eds.), Goodman and Gilman the Pharmacological Basis of Therapeutics, McGraw Hill, N.Y., 1996, pp. 1209–1263.
[2] S.A. Johnson, P. Harper, G.N. Hourobagyi, V.P. Pouillar, Vinorelbine: an overview, Cancer Treat. Rep. 22 (1996) 127–142.
[3] R.J. Toso, M.A. Jordan, K.W. Farrell, B. Matsumoto, Kinetic stabilization of microtubule dynamic instability in vitro by vinblastine, Biochemistry 32 (1993) 1285–1293.
[4] M.A. Jordan, D. Thrower, L. Wilson, Mechanism of inhibition of cell proliferation by vinca alkaloids, Cancer Res. 5 (1991) 2212–2222.
[5] G.C. Na, S.N. Timasheff, Thermodynamic linkage between tubulin self-association and the binding of vinblastine, Biochemistry 19 (1980) 1355–1365.
[6] S. Lobert, J. Fahy, B.T. Hill, A. Duflos, C. Entievant, J.J. Correia, Vinca alkaloid-induced tubulin spiral formation correlates with cytotoxicity in the leukemic L1210 cell line, Biochemistry 39 (2000) 12053–12062.
[7] S. Lobert, J.J. Correia, Energetics of vinca alkaloid interactions with tubulin, Methods Enzymol. 323 (2000) 77–103.
[8] S. Lobert, B. Vulevic, J.J. Correia, Interaction of vinca alkaloids with tubulin: a comparison of vinblastine vincristine and vinorelbine, Biochemistry 35 (1996) 6806–6814.
[9] S. Lobert, J.W. Ingram, B.T. Hill, J.J. Correia, A comparison of thermodynamic parameters for vinorelbine_ and vinflunine_induced tubulin self association by sedimentation velocity, Mol. Pharmacol. 53 (1998) 908–915.
[10] R.C. Williams Jr., J.C. Lee, Preparation of tubulin from brain, Methods Enzymol. 85 (1982) 376–408.
[11] J.J. Correia, L.T. Baty, R.C. Williams Jr., The Mg^{+2}-dependence of guanine nucleotide binding to tubulin, J. Biol.Chem. 262 (1987) 17278–17284.
[12] H.W. Detrich, R.C. Williams Jr., Reversible dissociation of the αβ dimer of tubulin from bovine brain, Biochemistry 17 (1978) 3900–3907.
[13] S. Lobert, A. Frankfurter, J.J. Correia, Binding of vinblastine to phosphocellulose-purified and αβ-class III tubulin: the role of nucleotides and β-tubulin isotypes, Biochemistry 34 (1995) 8050–8060.
[14] W.F. Stafford, Boundary analysis in sedimentation transport experiments: a procedure for obtaining sedimentation coefficient distributions using the time derivative of the concentration profile, Anal. Biochem. 203 (1992) 295–301.
[15] J.J. Correia, The analysis of weight average sedimentation data, Methods Enzymol. Numer. Comput. Methods, C 321 (2000) 81–100.
[16] B. Vulevic, J.J. Correia, Thermodynamic and structural analysis of microtubule assembly: the role of GTP hydrolysis, Biophys. J. 72 (1997) 1357–1375.
[17] J.J. Correia, S. Lobert, Physiochemical aspects of tubulin-interacting, antimitotic drugs, Curr. Pharm. Des. 7 (2001) 1213–1228.
[18] J. J. Correia, S. Lobert. Molecular Mechanisms of Micotubule Acting Cancer Drugs, Microtubules in Health and Disease (Ed., Tito Fojo), Humana Press, in press.
[19] S. Lobert, C.A. Boyd, J.J. Correia, Divalent cation and ionic strength effects on vinca alkaloid-induced tubulin self-association, Biophys. J. 72 (1997) 416–427.
[20] V. Prakash, S.N. Timasheff, Mechanism of interaction of vinca alkaloids with tubulin: catharanthine and vindoline, Biochemistry 30 (1991) 873–880.
[21] R.S. Spolar, J.R. Livingstone, M.T. Record, Use of liquid hydrocarbon and amide transfer data to estimate contributions to thermodynamic functions of protein folding from the removal of nonpolar and polar surface from water, Biochemistry 31 (1992) 3947–3955.
[22] R.S. Spolar, M.T. Record, Coupling of local folding to site-specific binding of proteins to DNA, Science 263 (1994) 777–784.
[23] A. Cooper, C.M. Johnson, J.H. Lakey, M. Nollmann, Heat does not come in different colours: entropy–enthalpy compensation, free energy windows, quantum confinement, pressure perturbation calorimetry, solvation and multiple causes of heat capacity effects in biomolecular interactions, Biophys. Chem. 93 (2001) 215–230.

[24] J.M. Sturtevant, The thermodynamic effects of protein mutations, Curr. Opin. Struck. Biol. 4 (1994) 69–78.
[25] C. Frisch, G. Schreiber, C.M. Johnson, A.R. Fersht, Thermodynamics of the interaction of Barnase and Barstar: changes in free energy versus changes in enthalpy on mutation, J. Mol. Biol. 267 (1997) 696–706.
[26] B. Gigant, C. Wang, R.B.G. Ravelli, F. Roussi, M.O. Steinmetz, P.A. Curmi, A. Sobel, M. Knossow, Structural basis for the regulation of tubulin by vinblastine, Nature 435 (2005) 519–527.
[27] K.M. Guthrie, A.D.C. Parenty, L.V. Smith, A. Cooper, Microcalorimetry of interaction of dihydro-imidazole-phenanthridinium (DIP)-based compounds with duplex DNA, Biophys. Chem. (2006) (this volume).
[28] R.A. Santarella, J.J. Correia, S. Lobert, A. Hoenger, Cryo EM studies of effects on microtubule structure by vinblastine-tau, Mol. Biol. Cell Suppl. 16 (2005) 957, CDRom.
[29] M.A. Jordan, R.L. Margolis, R.H. Himes, L. Wilson, Identification of a distinct class of vinblastine binding sites on microtubules, J. Mol. Biol. 187 (1986) 61–73.
[30] W.D. Singer, M.A. Jordan, L. Wilson, R.H. Himes, Binding of vinblastine to stabilized microtubules, Mol. Pharm. 36 (1989) 366–370.
[31] C. Iancu-Rubin, G.F. Atweh, $P27^{Kip1}$ and stathmin share the stage for the first time, Trends Cell Biol. 15 (2005) 346–348.